Mapping the Pharyngeal and Intestinal pH of *Caenorhabditis elegans* and Real-Time Luminal pH Oscillations Using Extended Dynamic Range pH-Sensitive Nanosensors

Veeren M. Chauhan,[†] Gianni Orsi,[‡] Alan Brown,[§] David I. Pritchard,[§] and Jonathan W. Aylott[†,*]

[†]Laboratory of Biophysics and Surface Analysis, School of Pharmacy, University of Nottingham, Boots Sciences Building, University Park, Nottingham, United Kingdom NG7 2RD, [‡]Research Centre "E.Piaggio", University of Pisa, Largo Lucio Lazzarino 1, 56126 Pisa, Italy, and [§]Immune Modulation, School of Pharmacy, University of Nottingham, Boots Sciences Building, University Park, Nottingham, United Kingdom NG7 2RD

ABSTRACT Extended dynamic range pH-sensitive ratiometric nanosensors, capable of accurately mapping the full physiological pH range, have been developed and used to characterize the pH of the pharyngeal and intestinal lumen of *Caenorhabditis elegans* in real-time. Nanosensors, 40 nm in diameter, were prepared by conjugating pH-sensitive fluorophores, carboxyfluorescein (FAM) and Oregon Green (OG) in a 1:1 ratio, and a reference fluorophore, 5-(and-6)-carboxytetramethylrhodamine (TAMRA) to an inert polyacrylamide matrix. Accurate ratiometric pH measurements were calculated through determination of the fluorescence ratio between the pH-sensitive and reference fluorophores. Nanosensors were calibrated with an automated image analysis system and validated to demonstrate a pH measurement resolution of ±0.17 pH units. The motility of *C. elegans* populations, as an indicator for viability, showed nematodes treated with nanosensors, for concentrations ranging from 50.00 to 3.13 mg/mL, were not statistically different to nematodes not challenged with nanosensors up to a period of 4 days ($p < 0.05$). The nanosensors were also found to remain in the *C. elegans* lumen >24 h after nanosensor challenge was removed. The pH of viable *C. elegans* lumen was found to range from 5.96 ± 0.31 in the anterior pharynx to 3.59 ± 0.09 in the posterior intestine. The pharyngeal pumping rate, which dictates the transfer of ingested material from the pharynx to the intestine, was found to be temperature dependent. Imaging *C. elegans* at 4 °C reduced the pharyngeal pumping rate to 7 contractions/min and enabled the reconstruction of rhythmic pH oscillations in the intestinal lumen in real-time with fluorescence microscopy.

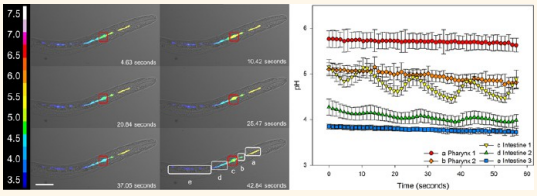

KEYWORDS: *C. elegans* · lumen · fluorescence · pH measurement · nanosensors · real-time · pH oscillations

Caenorhabditis elegans, nature's gift to science,[1] is a ubiquitous non-parasitic free living nematode. Because of its relative ease of growth and maintenance,[2] short life cycle,[3] and optical transparency, *C. elegans* has become a powerful tool to model complex biological processes such as genetics,[4,5] neurology,[6] cell survival,[7] and toxicology.[8] More recently, the *C. elegans* intestinal lumen has been highlighted as a suitable model to study digestion and metabolism to aid the discovery of new targets and therapeutics for acid suppression.[9]

C. elegans are typically cultured in the presence of *Escherichia coli* for sustenance. On ingestion, bacteria are rhythmically pumped from the anterior to the posterior pharynx where they are subjected to mechanical degradation by the pharyngeal grinder.[10] Pharyngeal pumping also permits the opening and closing of the pharyngeal-intestinal valve, approximately 300 times/min.[11] The opening of the pharyngeal-intestinal valve allows the transfer of ingested material from the pharynx to the intestinal lumen.[10] In the intestinal lumen, ingested matter is chemically metabolized into smaller fragments for intestinal uptake by digestive hydrolases.[12] The activity of *C. elegans* intestinal hydrolases is optimal in mildly acidic conditions.[13,14] This is important because *C. elegans* periodically expel undigested luminal contents approximately

* Address correspondence to jon.aylott@nottingham.ac.uk.

Received for review April 15, 2013 and accepted May 13, 2013.

Published online May 13, 2013
10.1021/nn401856u

every 45 s.[15] Therefore, the pH of the *C. elegans* intestine must be carefully regulated so that the digestive enzymes have an opportunity to breakdown proteins and carbohydrates before they are rapidly ejected from the lumen.[12] The pH of the *C. elegans* intestinal lumen is regulated by proton pumps,[16] exchangers and transporters[17] located on the apical membrane of the intestinal lumen. The vacuolar type adenosine triphosphatase (V-ATPase), in particular the V-ATPase containing the VHA-6 protein subunit, has been identified as the key proton pump responsible for the acidification of the *C. elegans* intestinal lumen.[18] The use of transgenic nematodes, expressing fluorescently labeled VHA-6,[16] and immunostaining, with fluorescently labeled anti-VHA-6 antibodies,[19] has also shown the V-ATPase containing VHA-6 subunit is heavily expressed at the pharyngeal-intestinal junction, the site where ingested material first enters the intestinal lumen and is exposed to digestive enzymes. Accurate determination of the *C. elegans* luminal pH would augment the understanding of the role proton pumps play in the activity of key luminal hydrolases.

Dextran bound pH-sensitive fluorophores, which demonstrate pH-dependent changes in fluorescence intensity, have been used to image the average pH across the *C. elegans* intestinal lumen.[16,20] The use of pH-sensitive dextran bound conjugates is however limited by the range, accuracy and duration of pH measurement. Typically, dextran bound pH-sensitive probes which utilize a single fluorescein based fluorophore are limited by the range of pH measurements that can be made[21] and are subject to concentration related artifacts due to the absence of ratiometric measurements.[22] Furthermore, ingested dextran bound fluorophores are rapidly excreted from the *C. elegans* lumen during defecation[20] and as a result are restricted to short sample preparation times when imaging using fluorescence microscopy and also limited by the duration of time pH measurement can be made across the length of the nematode. Probes which remain in the *C. elegans* lumen for an extended period of time, such as nanoparticles,[23] could be used to map luminal pH and the acidification of ingested material in real-time. An example of nanoparticles capable of making pH measurements are fluorescent pH-sensitive nanosensors.[24]

Fluorescent pH-sensitive nanosensors are spherical probes typically composed of a pH-sensitive fluorophore and a pH-insensitive reference fluorophore encapsulated or covalently linked to an inert porous cross-linked matrix.[25,26] The inert matrix shields the fluorophores from cellular components, which could hinder sensing capabilities, while safeguarding biological components from free fluorophores.[27] The combination of pH-sensitive and pH-insensitive fluorophores in a single nanoparticle enables accurate ratiometric pH measurements.[28] Nanosensors composed of fluorescein based pH-sensitive fluorophores, such as carboxyfluorescein (FAM) and Oregon Green (OG), when suspended in aqueous media, exhibit high and low fluorescent responses at near neutral and acidic pH values, respectively. This effect is due the pH-dependent ionic equilibria of fluorescein based fluorophores, which demonstrate high quantum yields when fully ionized, *e.g.*, in aqueous solutions greater than pH 8.0, and a diminished fluorescent response and quantum yields when protonated, *e.g.*, in aqueous solutions with a pH less than 3.0.[29]

Nanoparticles composed of a single pH-sensitive fluorophore, either FAM or OG, have a limited range of pH measurement, of pH ~ 5.00−7.50 and pH ~ 3.50−6.00, respectively.[30] In contrast, extended dynamic range pH-sensitive nanosensors, which combine FAM and OG in 1:1 ratio in a single nanosensor, are capable of measuring the full physiological pH range, from pH 3.50 to 7.50.[30−32]

The present article describes the characterization, validation and application of extended dynamic range pH-sensitive nanosensors to the measurement of pharyngeal and intestinal pH in *C. elegans*. The nanosensors were used to convert pH dependent changes in fluorescence intensity into quantifiable pH measurements, using an automated image analysis system. The nanosensors were assessed for their effect on *C. elegans* viability, in order to establish nanoparticle treatment time and concentration to maintain *C. elegans* viability during pH measurement. The nanosensors were successfully delivered to nematodes and used to map pH of the pharyngeal and intestinal lumen of *C. elegans in vivo*. In addition, through control of the pharyngeal pumping rate, the acidification of the intestinal lumen was mapped in real-time.

RESULTS AND DISCUSSION

Characterization of Extended Dynamic Range pH-Sensitive Nanosensors. Extended dynamic range pH-sensitive nanosensors[30] were prepared by covalently linking pH-sensitive (FAM and OG) and pH-insensitive (TAMRA) fluorophores to *N*-(3-aminopropyl)methacrylamide (APMA), which was then copolymerized with acrylamide and *N*,*N*′methylenebis(acrylamide) to produce an inert polyacrylamide nanoparticle matrix, Figure 1A. Nanosensors were sized using environmental scanning electron microscopy (ESEM) and dynamic light scattering (DLS) and shown to have a diameter of ~40 nm (see Supporting Information, Figure S3A, and 3B, respectively). FAM and OG are both excited at 488 nm for which they demonstrate a pH-dependent overlapping emission peak at ~520 nm, whereas TAMRA, when excited at 540 nm, exhibits a pH-independent fluorescence response at ~577 nm, Figure 1B. A ratiometric pH calibration curve can be generated, Figure 1C, by taking a ratio of the fluorescence response of pH-sensitive and pH-insensitive channels (λ_{em} 520 nm/λ_{em} 577 nm) from

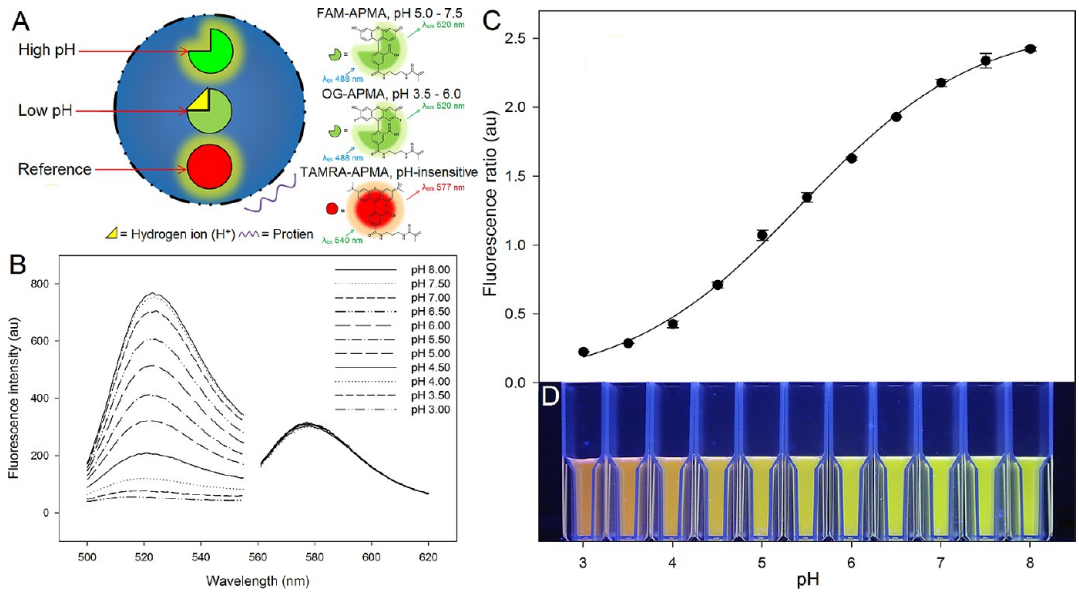

Figure 1. (A) Schematic diagram of extended dynamic range pH-sensitive nanosensors. (B) Emission curves and (C) calibration curve for pH-sensitive nanosensors suspended in buffer solutions ranging from pH 3.00 to 8.00. FAM-APMA and OG-APMA both excite and emit fluorescence at 488 nm and ~520 nm, respectively, whereas TAMRA-APMA excites and emits fluorescence at 540 nm and ~577 nm, respectively. Data points for the calibration curve are fitted to a sigmoidal expression, where error bars represent standard deviation ($pK_a = 5.44 \pm 0.07$). (D) Ultraviolet trans-illuminated pH-sensitive nanosensors (λ_{ex} 302 nm).

nanosensors suspended in a range of pH buffer solutions, Figure 1D. The calibration curve can then be used to make accurate ratiometric pH measurements from environments containing pH-sensitive nanosensors.

Synthesis of nanosensors with covalently linked fluorophores overcomes measurement inaccuracies associated with fluorophore leaching. Over time, nanosensors prepared through the encapsulation of dextran bound pH-sensitive fluorophores have been found to leach.[33] Nanosensors which leach fluorophores are subject to pH measurement artifacts, as the operator cannot be certain if pH measurements are being made from the nanosensors or free fluorophore.[34] Leached fluorophores could also initiate cellular toxicity due to photoexcitation and/or nonspecific protein binding.[27]

Nanosensors prepared with covalently linked fluorophores are also extremely bright when compared to nanosensors composed of encapsulated fluorophores.[35] Brighter nanosensors permit (1) a reduction in fluorescence excitation energy, preserving biological function and reduced fluorophore photobleaching;[36] (2) use of lower nanosensor concentrations for measurement; and (3) a reduction in the required exposure time of fluorescence microscopy, permitting faster imaging of dynamic process through increases in sampling rate.

Nanosensors and *C. elegans* Viability. Motility of *C. elegans* can be used to predict aging,[37,38] lifespan,[39] survival and/or viability.[40] In general, nematode body movement gradually declines and stops completely with age.[41] Through use of *C. elegans* motility as an absolute parameter, where motile and nonmotile nematodes were classified as viable and nonviable, respectively, the effect of suspending nematodes in range of concentrations of extended dynamic range pH-sensitive nanosensors was explored. To ensure continual exposure to nanosensors for the duration of study, synchronized L_1-L_2 staged nematodes, supplemented with *E. coli* OP50 for sustenance, were suspended in a liquid culture of serially diluted nanosensor suspensions, ranging from 50.00 to 3.13 mg/mL. *C. elegans* suspended with *E. coli* alone were used as a negative control. Motile (viable) and nonmotile (nonviable) worms were counted daily, by acquiring an aspirated sample from a nematode-nanosensor sensor suspension. Aspiration enabled agitation of nematodes so that viable nematodes would demonstrate a motile response when counted. Counted nematodes were returned to the stock suspensions. The motile fraction (*Mf*) was calculated by taking a ratio of the number of motile nematodes (M) at a time point (t) by the total number of nematodes counted (sum of motile (M_t) and nonmotile nematodes (N_t)), as described in eq 1.

$$Mf_t = \frac{M_t}{M_t + N_t} \quad (1)$$

The *Mf*, as an indicator for *C. elegans* viability, showed untreated populations of nematodes were motile for approximately 20 ± 1 days, which is comparable to previously reported survivorship data.[42] Furthermore, the *Mf*'s of *C. elegans*, when comparing nematodes treated with extended dynamic range pH-sensitive nanosensors with nontreated *C. elegans*, were not statistically different at all concentrations for up to 4 days

($p < 0.05$), Figure 2. To determine the effect of nanosensor concentration on nematode viability, the motility fraction half-life (Mft_{50}), the time required to reduce the motility of population of nematodes by 50%, was derived for each concentration of nanoparticles (see Supporting Information, Figure S4). The Mf_{t50} indicates *C. elegans* exhibit dose dependent decrease in viability, such that nematodes treated with greater concentrations of nanosensors were viable for shorter periods of time.

For our experiments high nanosensor concentrations are preferred, because they permit the maintenance of optimal signal-to-noise ratios, so that exposure times can be reduced and sampling rate increased when making pH measurements. However, high nanosensor concentrations have shown to reduce the viability of *C. elegans* over extended time periods. A compromise was established to maintain an optimal fluorescent signal-to-noise ratio, by using relatively high nanosensor concentrations, while preserving nematode viability, through reduction in treatment time.

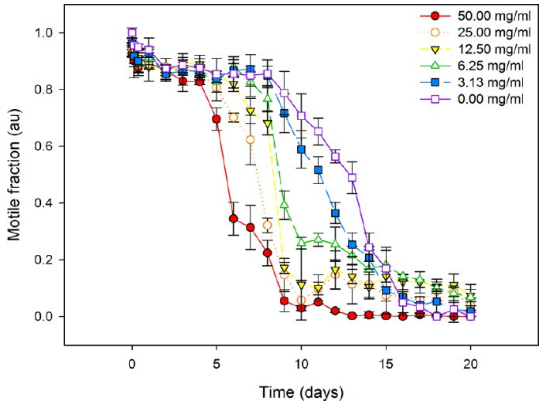

Figure 2. Motile fraction (*Mf*) of *C. elegans* when exposed to extended dynamic range pH-sensitive nanosensors at concentrations ranging from 50.00 to 0.00 mg/mL, where error bars represent standard deviation. The experiment described above was conducted in triplicate and approximately 300 nematodes were surveyed for each time point and concentration.

Figure 3 shows a representative population of *C. elegans* with nanosensors distributed throughout the *C. elegans* pharyngeal and intestinal lumen, when imaged 24 h after treatment with nanosensors at a concentration of 30 mg/mL for 3 h. When the time of imaging and the relatively fast nematode defecation cycle are considered,[43] Figure 3 suggests the nanosensors could be adsorbing to the pharyngeal and intestinal lumen of *C. elegans*. This property of extended dynamic range pH-sensitive nanosensors is advantageous when compared to dextran bound fluorophores which are rapidly excreted from the *C. elegans* lumen.[20] This allows observation of dynamic processes, such as the transfer and acidification of intestinal contents, over extended time periods, which would otherwise not be possible with rapidly ejected fluorophores.

Development and Validation of Automated pH Image Analysis. Interpretation of data from imaging can be variable and open to subjective input from the operator especially when handing large volumes of data.[44,45] To overcome these challenges, an automated image processing system, independent of the operator, was created. The system is programmed to analyze images used for calibrating pH-sensitive nanosensors and then use this information to transform images for analysis to pH images for measurement.

Calibration images were analyzed, by taking a pixel-wise ratio of green and red fluorescent channels to

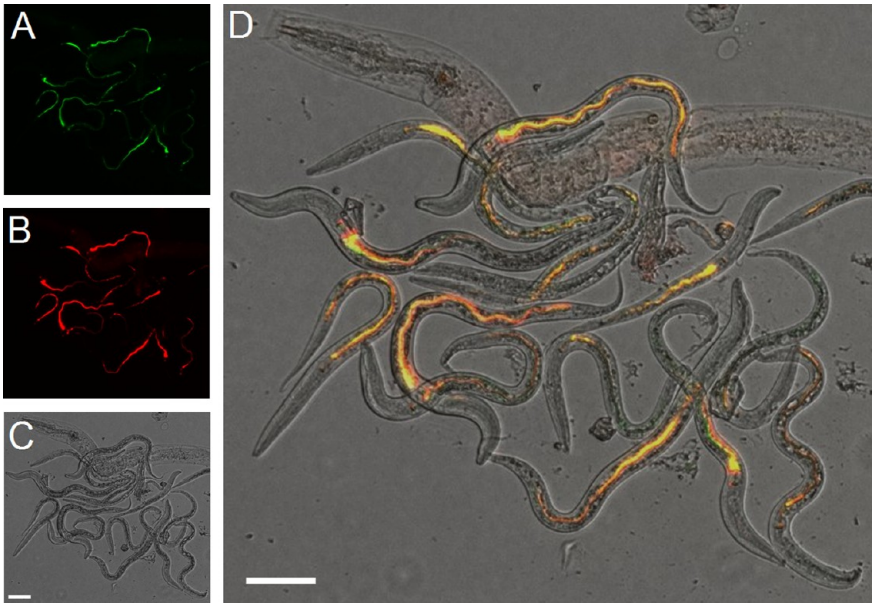

Figure 3. Population of *C. elegans* imaged in (A) green, (B) red, and (C) transmitted light channels, to produce a (D) merged channel image, after exposure to extended dynamic range pH-sensitive nanosensors (30 mg/mL) for 3 h. Nematodes were imaged 24 h after nanosensor challenge was removed. Scale bar = 50 μm.

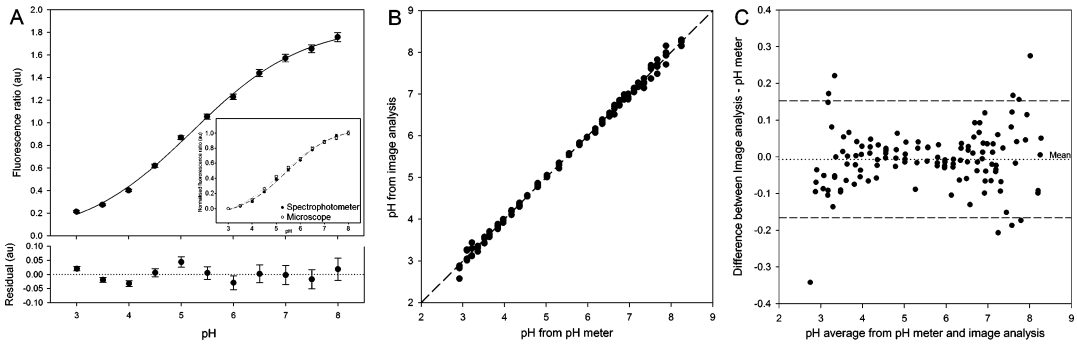

Figure 4. (A) pH calibration for extended dynamic range pH-sensitive nanosensors and residual error, when imaged using fluorescence microscopy. (Inset) Comparison of normalized calibration curves from peak fluorescent intensity from fluorescence spectrophotometer and high-throughput analysis of pH calibration images. (B) Comparison of pH measurements made with pH meter and image analysis of pH calibration images. (C) Bland-Altman mean difference plot used to demonstrate agreement between pH measurements made with image analysis and pH meter where dashed lines and dotted lines represent 95% confidence intervals and mean of plotted data, respectively.

obtain calibration points (I) from which a calibration curve was generated, Figure 4A (see Supporting Information). Calibration curves are fitted to a sigmoidal function, as described in eq 2,

$$I(\mathrm{pH}) = R_{\min} + \frac{R_{\max} - R_{\min}}{1 + e^{[(pK_a - \mathrm{pH})/b]}} \qquad (2)$$

where, R_{min} and R_{max} are the minimum and maximum fluorescent ratio, pK_a represents the pH at which the fluorophore exhibits its greatest sensitivity to changes in pH, and the slope factor b represents the sensitivity of the nanosensor to changes in pH.[30] Calibration curves generated from analysis of data from spectrophotometer and pH measurements made using a pH meter were used to validate the automated the image analysis system and used to determine the accuracy of extended dynamic range pH-sensitive nanosensors to make pH measurements.

Figure 4A *inset* shows normalized ratiometric calibration curves from both peak fluorescence intensity from fluorescence spectrophotometer and high throughput methods using fluorescence microscope. Statistical analysis of both curves indicates there are no significant differences between the calibrations curves ($p < 0.05$) and have comparable pK_a values of 5.36 $\pm$ 0.16. Furthermore, Figure 4B confirms pH measurements made using the high-throughput image analysis system are not statistically different to pH measurements made with the pH meter ($p < 0.05$). The Bland-Altman mean difference plot, Figure 4C, also demonstrates concordance between the two methods,[46] such that between pH 3.50 and 7.50 the 95% confidence interval remains between $\pm$0.17 pH units, which could be taken to be the pH measurement resolution.

Ratiometric analysis of motile *C. elegans* is challenging as the nematode under observation will on occasion move while being imaged, leading to nonregistration between the green and red fluorescent channels. Therefore, prior to transformation of green and red fluorescent channels to pH images, co-localization

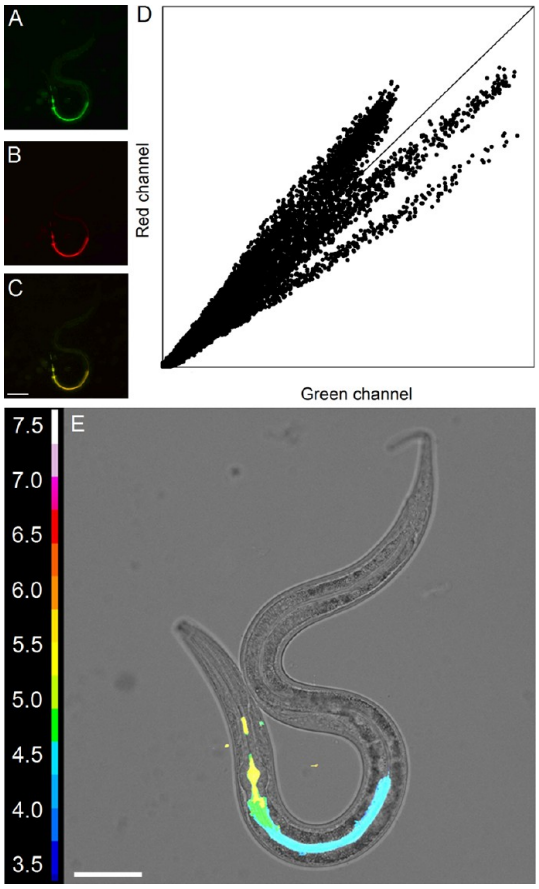

Figure 5. (A) Green, (B) red, and (C) merged fluorescence microscopy images of *C. elegans* with ingested extended dynamic range pH-sensitive nanosensors. (D) Co-localization analysis of green and red channels (Pearson's correlation coefficient = 0.98). (E) Transformed false color pH heat map image. Scale bar = 50 μm.

analyses were performed to ensure co-registration of fluorescent channels. Through visual inspection of green, red, and merged channel images, Figure 5A–C, and co-localization analyses, Figure 5D, images with a Pearson's Correlation Coefficient of greater than 0.95 were taken forward for pH measurement.

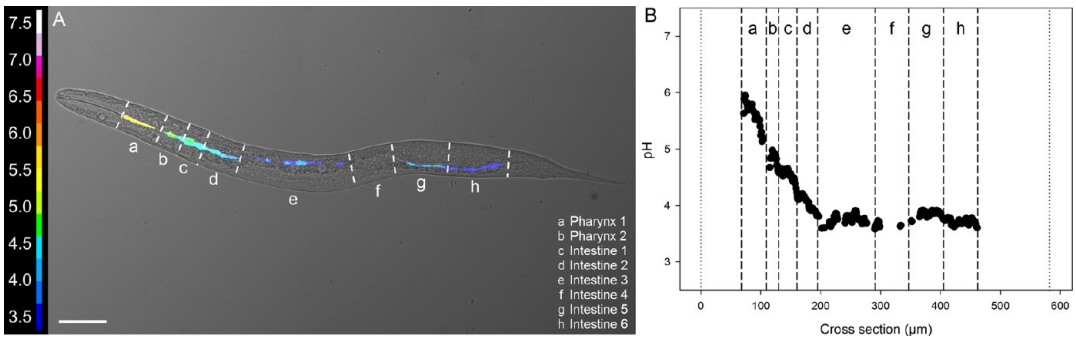

Figure 6. (A) Transformed pH-image of *C. elegans*, with ingested extended dynamic range pH-sensitive nanosensors, and (B) corresponding pH values. For data containing standard deviation of measured pH see Supporting Information, Figure S5A. Dotted lines at 0 and 582 μm represent start of head and end of tail of *C. elegans*. Scale bar = 50 μm.

A ratiometric image was generated by taking a pixel-wise ratio of green and red fluorescent channels (Figure 5A,B) to produce a gray scale image which was transformed into a false color pH heat map, Figure 5E (see Supporting Information for detailed methodology).

Mapping the Pharyngeal and Intestinal pH of *C. elegans*. Viable nematodes with ingested extended dynamic range pH-sensitive nanosensors exhibit a pH gradient from pharynx to tail. Figure 6A shows a representative pH-image of a *C. elegans* nematode with ingested nanosensors. The lumen of *C. elegans* has been segmented into areas which visually appear to be similar in pH. The calculated pH values, Figure 6B, show the intestinal pH ranges from pH 5.96 $\pm$ 0.31 in the pharynx to 3.59 $\pm$ 0.09 in the intestine. The average pharyngeal pH was found to be pH 5.35 $\pm$ 0.26, whereas the average intestinal pH of *C. elegans* was found to be pH 3.92 $\pm$ 0.22. Further analysis of Figure 6B highlights that the pH of the lumen decreases from the upper regions of the nematode, from *Pharynx 1* to *Intestine 2*, after which the intestinal regions, from *Intestine 3* to *Intestine 6*, exhibit an average of pH 3.77 $\pm$ 0.08. V-ATPases found at the pharyngeal-intestinal junction, located between *Pharynx 2* and Intestine *1*, are postulated to be essential for the rapid acidification of ingested material, Figure 6A.[19]

Conversely, nonviable nematodes do not maintain a pH gradient from the anterior of the pharynx to the posterior of the intestinal lumen Figure 7A. Figure 7B shows the average luminal pH of nonviable *C. elegans* was found to be 5.95 $\pm$ 0.12, which is comparable to the pH of the surrounding media and the pharynx of viable nematodes. Comparison of viable and nonviable nematodes, through normalization of nematode anatomy, highlights differences in luminal pH, Figure 7B *inset*. The differences seen in the luminal pH of viable and nonviable *C. elegans* could be due the inability to regulate the opening and closing of the pharyngeal-intestinal valve and/or the loss of function of intestinal proton pumps in the nonviable nematode.

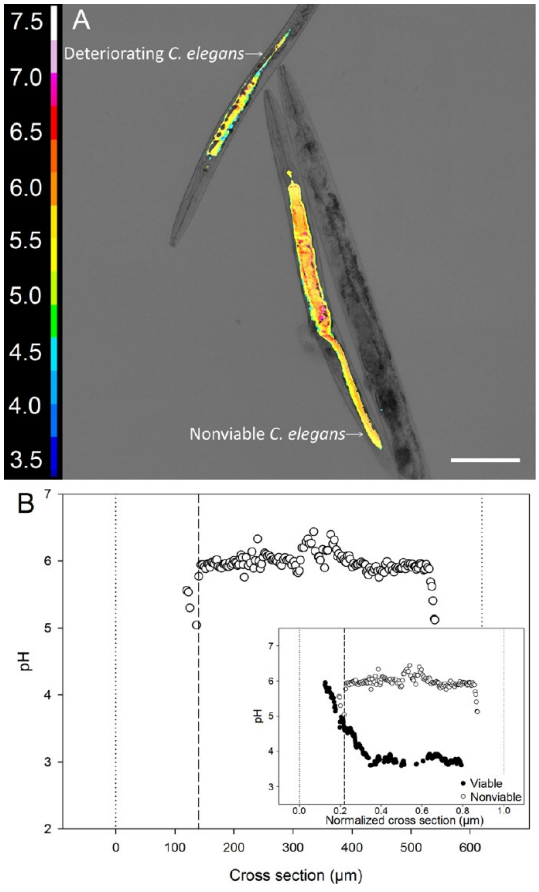

Figure 7. (A) pH image of nonviable *C. elegans* alongside a deteriorating nematode and a nonviable *C. elegans*, which has not ingested nanosensors. (B) Luminal pH values for nonviable nematodes and (inset) comparison of viable and nonviable *C. elegans* luminal pH, through normalization of worm anatomy. For data containing standard deviation of measured pH see Supporting Information, Figure S5. Dotted lines represent start of head and end of tail of nematode. Dashed line represents location of pharyngeal-intestinal junction. Scale bar = 100 μm.

The data presented above suggests that the capacity of the apical cells to acidify the anterior of the intestinal lumen is large when the rapid expulsion ingested contents and digestive enzymes are taken into account. The peak activity of key intestinal

hydrolases, such as aspartyl-proteases and acid-phosphatases, has been found to be at pH 5[47] and 4,[14] respectively, which could suggest optimal activity of different hydrolases may occur at different regions of *C. elegans* intestinal lumen. The region of the intestine which has been thought to contain the majority of proton pumps,[19] *Intestine 1*, is also found at the center of the region of the nematode with decreasing pH (Figure 6A, regions a−d). This may imply *C. elegans*, like mammals,[48] could also be susceptible to acid reflux as the pharyngeal regions are also subjected to acidic pH during pharyngeal pumping.

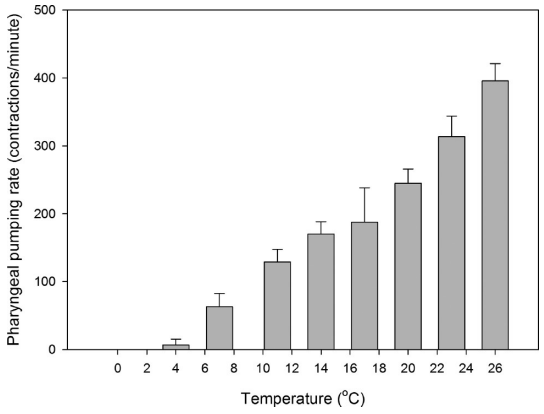

Figure 8. Temperature dependent changes in *C. elegans* pharyngeal pumping rate (contractions/minute). Error bars represent standard deviation (n = 20).

Real-Time *in Situ* Mapping of Rhythmic pH Oscillations in the *C. elegans* Lumen. Imaging the acidification of lumen contents, at the pharyngeal-intestinal junction, in real-time at 20 °C is challenging. The sampling theorem states a sampling rate of least twice the signal/response is required to reconstruct a signal.[49] At 20 °C the pharyngeal pumping rate of a larval staged *C. elegans* is ∼300 contractions/min,[11] whereas a high speed automated fluorescent microscope can typically

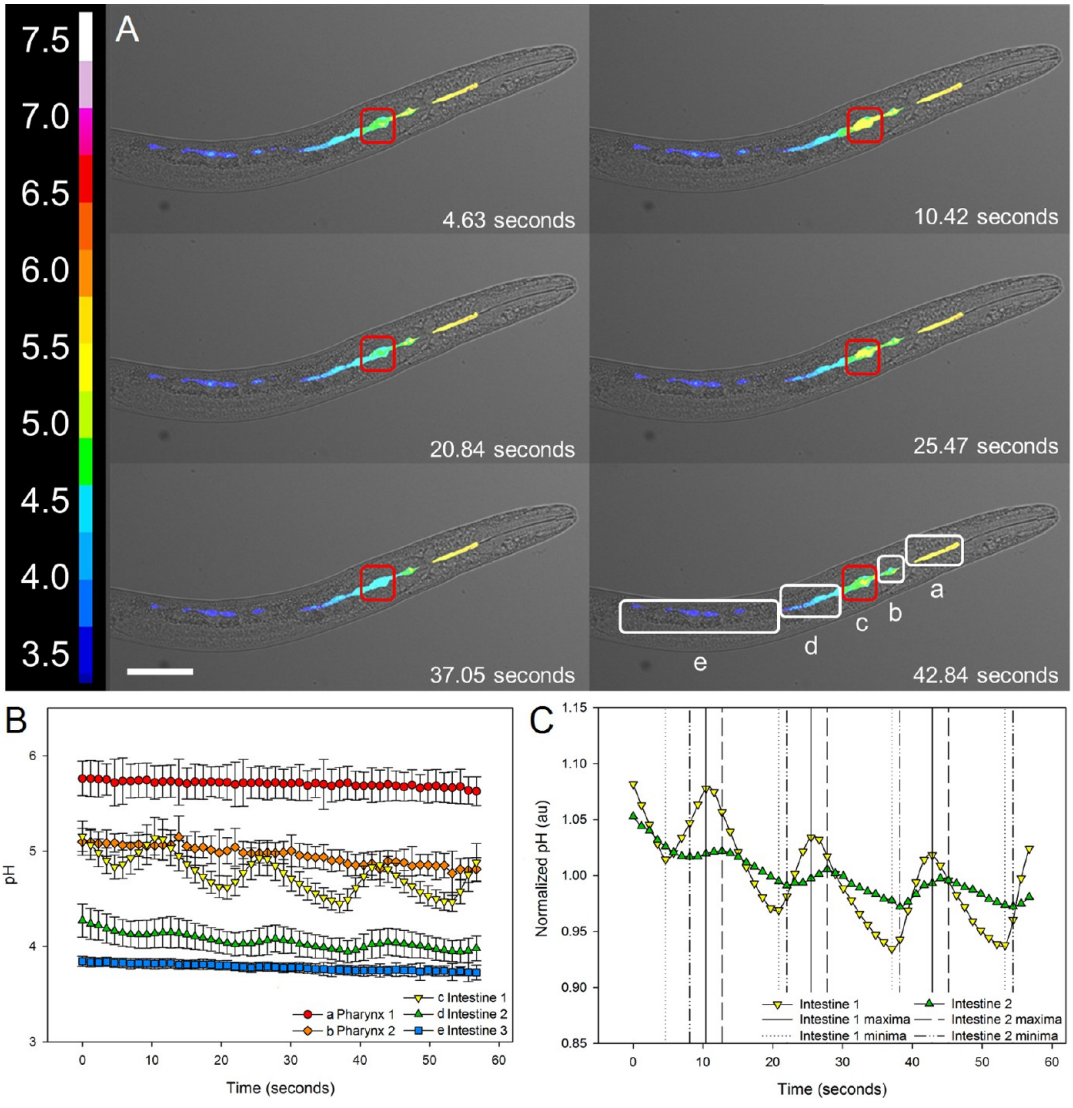

Figure 9. (A) Cross section of *C. elegans* at a peak (10.42, 25.47, and 42.84 s) and trough (4.63, 20.84, and 37.05 s) pH oscillations. (B) Measured and (C) normalized changes in pH over time. Regions a and b correspond to *Pharynx 1* and *Pharynx 2*, whereas regions c to e correspond to *Intestine 1* to *Intestine 3*. Error bars represent standard deviation of sampling area. Scale bar = 50 μm.

acquire three channels (green, red, and transmitted light) to generate a pH image at a rate of ~60 images/min. This implies that to reconstruct a pH oscillatory signal due to the opening and closing of the pharyngeal-intestinal valve the minimum sampling rate required at 20 °C is 600 images/min. Therefore, the pharyngeal pumping rate was investigated to establish if it can be controlled by changes in temperature.

Nematodes were equilibrated to range of different temperatures, between 0 and 26 °C, and the number of pharyngeal contractions at each temperature were counted over a 60 s interval, Figure 8. *C. elegans* were found to have a temperature dependent pumping rate, such that the pumping rate is ~50 times greater at 26 °C when compared to nematodes at 4 °C. Therefore, by imaging *C. elegans* at 4 °C, rather than 20 °C, the sampling rate would be ~8 times greater than the pharyngeal pumping rate, which would permit the real-time observation of the acidification of pharyngeal contents in the intestinal lumen using our imaging system.

Figure 9A shows a series of pH images of a representative nematode, with ingested nanosensors, imaged for a 60 s interval at 4 °C (see Supporting Information for time-lapse video). Regions of interest were selected, within the pharyngeal and intestinal lumen, which visually appear to be a similar in pH. The pH of these selected regions was mapped over time, Figure 9B. The pH values of the pharynx, *Pharynx 1* and *Pharynx 2*, are constant at pH of 5.71 ± 0.18 and 4.95 ± 0.13, respectively. Periodic oscillations in pH were observed in the anterior regions of the nematode intestinal lumen, *Intestine 1*, at the pharyngeal-intestinal junction. The pH oscillates from a trough of 4.63 ± 0.11 to a peak of 4.97 ± 0.18 every 5.40 ± 0.67 s, whereas the change from high to low pH, the acidification of pharyngeal contents, takes place every 10.81 ± 0.67 s. The pH of *Intestine 1* does not rise above the pH of *Pharynx 2*, which indicates pharyngeal contents are being acidified in the anterior intestine due to the regular rhythmic opening and closing of the pharyngeal-intestinal valve.

The pH of *Intestine 2* also oscillates with time from low to high pH every 5.78 ± 1.15 s and from high to low pH every 9.64 ± 0.67 s. However, the corresponding peaks and troughs observed in *Intestine 1* to *2* are lagged by 1.93 ± 0.67 and 1.73 ± 1.15 s, respectively, Figure 9C. Therefore, when comparing the oscillations observed in *Intestine 1* and *2*, a similar period of time is required to acidify and raise the pH of luminal contents in *Intestine 2*. However, the pH cycle is delayed by ~2 s which could be due to of peristaltic movement of ingested material from the anterior to the posterior regions of the *C. elegans* intestinal lumen.

CONCLUSION

We have demonstrated how extended dynamic range pH-sensitive nanosensors can be applied to the model organism *C. elegans* and be used to map the pH of the pharyngeal and intestinal lumen in real-time. Nanosensors were characterized for size and pH dependent changes in fluorescence intensity using fluorescence spectroscopy and an automated image analysis system. Validation of the automated image analysis system demonstrates the measurements made with nanosensors are comparable to those made with a pH meter and highlight the pH measurement resolution to be ±0.17 pH units. Assessment of the toxicity of *C. elegans* treated with nanosensors are not significantly different to untreated nematodes for up to 4 days, after which nematodes demonstrate a dose dependent decrease in viability. Maintenance of *C. elegans* viability while obtaining optimal imaging parameters was achieved through reduction in nanosensor treatment time and the use of high nanosensor concentrations, which permit the increases in the sampling rate. Nanosensors were found to remain in the *C. elegans* pharyngeal and intestinal lumen after nanosensor challenge was removed for >24 h. This enabled longer sample preparation times and enhanced duration of pH measurement such that the acidification of the intestinal lumen could be mapped in real-time. The pH of viable *C. elegans* was found to form a gradient from the pharyngeal to the intestinal lumen, where pH ranged from 5.96 ± 0.31 to 3.59 ± 0.09, respectively. Nonviable *C. elegans* were not able to maintain a pharyngeal and intestinal luminal pH gradient, such that the luminal pH reflected that of the surrounding media. This could be due to the inability of nonviable nematodes to control the opening and closing of the pharyngeal-intestinal value and/or loss of function of the luminal proton pumps.

To map the acidification of the pharyngeal contents in the intestinal lumen, the rate of pharyngeal pumping was reduced by lowering the temperature surrounding the nematodes. While maintaining a high sampling rate, the pH oscillations which indicate the acidification of intestinal lumen were reconstructed by imaging *C.elegans* at 4 °C. Oscillations in pH at the anterior of the intestinal lumen, which correspond to transfer of high pH pharyngeal contents into the intestinal lumen and the acidification of lumen contents by proton pumps, were found to occur at regular rhythmic intervals. These oscillations were also observed in latter parts of the intestinal lumen at lagged time points which may suggest peristaltic movement of ingested luminal contents.

We envisage extended dynamic range pH-sensitive nanosensors could prove to be a powerful tool to enhance our understanding of nematode pharyngeal and intestinal lumen[50] and the role pH plays in disease progression and therapeutic efficacy.

METHODS

Extended Dynamic Range pH-Sensitive Nanosensor Synthesis. Surfactants Brij 30 (3.080 g, 8.508 mmol), dioctyl sodium sulfosuccinate salt (1.590 g, 3.577 mmol) and deoxygenated hexane (42 mL) were stirred under argon for 10 min. Succinimidyl esters forms of the fluorophores were conjugated to APMA, *via* a nucleophilic addition reaction (see Supporting Information, Figure S1). FAM-APMA (15 μL, 5 mg/mL), OG-APMA (15 μL, 5 mg/mL), TAMRA-APMA (60 μL, 5 mg/mL), acrylamide (0.540 g, 7.579 mmol), and *N*,*N*′methylenebis(acrylamide) (0.160 g, 1.307 mmol) were dissolved in deionized water made up to 2 mL. This monomer solution was added to the stirring hexane surfactant solution and allowed to deoxygenate for a further 10 min. Polymerization initiators ammonium persulfate (30 μL, 10% w/v) and *N*,*N*,*N*′,*N*′-tetramethylethylenediamine (15 μL, 0.1 mmol) were added to the stirring solution to initiate polymerization. The mixture was left to stir for 2 h under argon. Hexane was removed *via* rotary evaporation. Nanoparticles were precipitated and washed with ethanol (30 mL) using centrifugation (10 times, 6000 rpm, 10 min), with a Hermle centrifuge (Z300). After the final wash, the pellet was resuspended in a small amount of ethanol (10 mL) and rotary evaporated until dry. Nanoparticles were stored in a light protected container at 4 °C.

***C. elegans* Growth, Maintenance, and Nanoparticle Challenged Viability.** *Growth and Maintenance.* *C. elegans* nematodes (Bristol N2) were maintained on nematode growth medium (NGM) agar[2] and *E. coli* (OP50) at 20 °C. Synchronized growth cycles of *C. elegans* were prepared by harvesting eggs from gravid females.[2] Briefly, a large number of gravid nematodes were collected by rinsing a NGM growth plate with sterile deionized water (3.5 mL). Sodium hydroxide (5 M, 0.5 mL) and sodium hypochlorite (5%, 1 mL) were added to the worm suspension and vortexed (10 min) to separate nematodes from the eggs. The eggs were initially collected using centrifugation (1500 rpm, 1 min), and subsequently washed once with 5 mL of sterile deionized water and collected with centrifugation (1500 rpm, 1 min). The centrifuged egg suspension was aspirated to 0.1 mL and plated onto a fresh plate of NGM agar, seeded overnight with an *E. coli* lawn. The generation time of *C. elegans* using these conditions was 4 to 5 days.

Nanoparticles and Nematode Viability. NGM agar plates containing synchronized cycles of *C. elegans* (L_1-L_2 larval stages) were harvested using sterile M9 buffer solution.[2] The nematodes were washed with sterile M9 buffer (1 mL, 3 times) and collected using centrifugation (1500 rpm, 1 min). The nematode suspension was diluted with sterile M9 buffer, containing *E. coli* OP50 (OD_{600nm} = 1.042, ~8×10^8 CFU) for sustenance, to a concentration of ~6000 nematodes/mL. Aliquots of this worm stock solution (0.100 mL) were added to a microtiter plate containing serially diluted pH-sensitive nanosensors, suspended in sterile M9 buffer solution (0.100 mL). Concentrations of pH-sensitive nanosensors used to dose *C. elegans* (~300 nematodes/0.200 mL) were 50.00, 25.00, 12.50, 6.25, and 3.13 mg/mL as well as a 0.00 mg/mL negative control (n = 3). Microtiter plates were continually oscillated (20 rpm, 20 °C) for duration of study. Motile and nonmotile nematodes were counted, using a dissecting microscope (Nikon Eclipse TS100, Nikon 4× 0.10 NA (air) objective), using a 0.100 mL sample from each well and returned once counting was complete. Motile nematodes were classified as viable, whereas, nonmotile nematodes were classified as nonviable. Initially *C. elegans* were counted at 0, 3, 6, and 9 and 24 h then every 24 h until the negative control nematodes were no longer motile. One way analysis of variance (ANOVA), followed by Dunnett's multiple comparison test, was performed for each time point and concentration of nanoparticles used to determine if nematode survival was comparable to untreated nematodes (α = 0.05).

Validation of pH Measurement. In plane focused images (n = 4) of nanosensors suspended in buffer solutions (n = 31), ranging from pH 2.92 to 8.25 were acquired for measurement validation using an automated image analysis system (see Supporting Information). Student's t test was used to identify significant differences between measurements made with image analysis system and fluorescence spectrophotometer, and image analysis and pH meter. Measurements made using the automated image analysis system were compared to measurements made from a pH meter (Jenway 3510) and used to determine a method resolution using 95% confidence intervals on a Bland-Altman mean difference plot (Sigma-Plot 12.0). Co-localization analyses were performed using the *Coloc 2* macro on FIJI open source software, from which images with Pearson's correlation coefficients, for green and red fluorescent channels, greater than 0.95 were taken for pH measurement.

Imaging *C. elegans* Luminal pH with Extended Dynamic Range pH-Sensitive Nanosensors. *C. elegans* nematodes were harvested from synchronized NGM growth plates using M9 buffer solution (1 mL, 3 times) and collected using centrifugation (1500 rpm, 1 min). The collected nematodes were suspended in M9 buffer containing extended dynamic range pH-sensitive nanosensors (0.5 mL, 30 mg/mL), seeded with *E. coli* OP50. *C. elegans* were allowed to ingest the pH-sensitive nanosensors for a period of 3 h at 20 °C. Hereafter, they were again washed with sterile deionized water, to remove any remaining noningested nanosensors and *E. coli*, and collected with centrifugation, as described above. The pelleted *C. elegans* were suspended in a small volume of sterile deionized water and transferred to poly-L-lysine coated glass bottom dishes. The small volume of water surrounding the nematodes was aspirated and the worms were trapped with a thin layer of pregelled agarose hydrogel (2%, at 4 °C). The poly-L-lysine and agarose were used to restrict *C. elegans* movement during imaging. Nematode movement can hinder image acquisition as a result of shifting transmitted light and fluorescent channels. Imaging acidification of *C. elegans* was achieved by compressing nematodes with a refrigerated agarose layer (4 °C). The temperature was continually monitored with a Digitron temperature gun (630−670 nm, < 1 mW).

A DeltaVision Elite (Applied Precision) with Olympus IX71 stand inverted microscope coupled with an Olympus U-Plan S-Apo 20× 0.85 NA (oil, Refractive index 1.520) and U-PlanFL N 10× 0.30 NA (air) objectives were used to image *C. elegans* and ingested extended dynamic range pH-sensitive nanosensors. A CoolSNAP *HQ*^{2} charged coupled device camera (6.45 × 6.45 μm pixel cell, 1000 kHz), interfaced Resolve3D softWoRx Acquire (version 5.5.0) software was used to acquire images (1024 × 1024, pixel size 0.331 × 0.331 × 0.200 μm). An InsightSSI solid state fluorescence light source was used to excite green fluorescence and red fluorescence at 475/28 nm (54 mW) and 542/27 nm (85 mW), respectively, while collecting emitted fluorescence, using a polychroic quad mirror in a sequential manner, at 523/36 and 594/45 nm, respectively. Transmission intensity and exposure times for green, red, and transmitted light used were 10%, 10% ,and 32%, respectively, and 0.025, 0.010, and 0.010 s, respectively. Acquired images were processed using MATLAB software and FIJI open source software (see Supporting Information). Regions of interest 9 μm wide which span the differing lengths perpendicular to the *C. elegans* pharyngeal and intestinal lumen were used to obtain average pH values and standard deviation across the length of the nematode lumen (see Supporting Information, Figure S5).

Controlling *C. elegans* Temperature Dependent Pharyngeal Pumping Rate. Populations of *C. elegans*, cultured on NGM plates, were subjected to a range of temperatures between 0 and 26 °C. The nematodes were allowed to equilibrate to the set temperatures

(30 min), which were recorded using a Digitron temperature gun (630−670 nm, <1 mW). Pharyngeal contractions were observed, using a dissecting microscope (Nikon Eclipse TS100, Nikon 20× 0.40 NA (air) objective) over a 60 s interval for each nematode in the study (n = 20). The average and standard deviation for pharyngeal contractions were determined for each temperature.

Conflict of Interest: The authors declare no competing financial interest.

Supporting Information Available: Detailed list of experimental materials. Methods for: (1) conjugation of succinimidyl ester fluorophores to APMA, (2) characterization and calibration of pH-sensitive nanosensors using fluorescence spectrophotometer, (3) derivation of motility fraction half-life (Mft_{50}) and (4) automated image analysis. Additional results showing the (1) ESEM and DLS of nanoparticles, (2) calculated Mft_{50} values, (3) luminal pH of viable and nonviable *C. elegans* with standard deviation, and (4) time-lapse video showing the acidification of intestinal lumen. This material is available free of charge *via* the Internet at http://pubs.acs.org.

Acknowledgment. The authors gratefully acknowledge Dr. Colin Berry and Cardiff University for donation of *C. elegans* (Bristol N2) and *E. coli* (OP50). The authors also acknowledge Leigh-Anne F. Carroll for help with ESEM, as well as Sarah-Jane Rymer and Dr. Emma M. King (Advanced Microscopy Unit, University of Nottingham) for helpful discussions. This research is supported by funding from a Biotechnology and Biosciences Research Council (BBSRC) CASE studentship (V.M.C.) (grant number BG0176381).

REFERENCES AND NOTES

1. Brenner, S. Nature's Gift to Science (Nobel Lecture). *ChemBioChem* **2003**, *4*, 683–687.
2. Stiernagle, T. Maintenance of *C. elegans*. In *WormBook: The Online Review of C. elegans Biology*; Wormbook: Pasadena CA, 2006; pp 1−11.
3. Byerly, L.; Cassada, R. C.; Russell, R. L. Life-cycle of Nematode *Caenorhabditis elegans* 0.1. Wild-Type Growth and Reproduction. *Dev. Biol.* **1976**, *51*, 23–33.
4. Brenner, S. Genetics of *Caenorhabditis elegans*. *Genetics* **1974**, *77*, 71–94.
5. Fire, A.; Xu, S. Q.; Montgomery, M. K.; Kostas, S. A.; Driver, S. E.; Mello, C. C. Potent and Specific Genetic Interference by Double-Stranded RNA in *Caenorhabditis elegans*. *Nature* **1998**, *391*, 806–811.
6. Chalfie, M.; Tu, Y.; Euskirchen, G.; Ward, W. W.; Prasher, D. C. Green fluorescent Protein as a Marker for Gene-Expression. *Science* **1994**, *263*, 802–805.
7. Adams, J. M.; Cory, S. The Bcl-2 Protein Family: Arbiters of Cell Survival. *Science* **1998**, *281*, 1322–1326.
8. Leung, M. C. K.; Williams, P. L.; Benedetto, A.; Au, C.; Helmcke, K. J.; Aschner, M.; Meyer, J. N. *Caenorhabditis elegans*: An Emerging Model in Biomedical and Environmental Toxicology. *Toxicol. Sci.* **2008**, *106*, 5–28.
9. Walker, G.; Houthoofd, K.; Vanfleteren, J. R.; Gems, D. Dietary Restriction in *C. elegans*: From Rate-of-Living Effects to Nutrient Sensing Pathways. *Mech. Ageing Dev.* **2005**, *126*, 929–937.
10. Avery, L.; Thomas, J. H. Feeding and Defecation. *Cold Spring Harbor Monogr. Ser.* **1997**, *33*, 679–716.
11. Huang, C.; Xiong, C. J.; Kornfeld, K. Measurements of Age-Related Changes of Physiological Processes that Predict Lifespan of *Caenorhabditis elegans*. *Proc. Natl. Acad. Sci. U. S.A.* **2004**, *101*, 8084–8089.
12. McGhee, J. D. The *C. elegans* Intestine. In *WormBook: The Online Review of C. elegans Biology*; Wormbook: Pasadena, CA, 2007; pp 1−36.
13. Sarkis, G. J.; Kurpiewski, M. R.; Ashcom, J. D.; Jenjacobson, L.; Jacobson, L. A. Proteases of the Nematode *Caenorhabditis elegans*. *Arch. Biochem. Biophys.* **1988**, *261*, 80–90.
14. Beh, C. T.; Ferrari, D. C.; Chung, M. A.; McGhee, J. D. An Acid-Phosphatase as a Biochemical Marker for Intestinal Development in the Nematode *Caenorhabditis elegans*. *Dev. Biol.* **1991**, *147*, 133–143.
15. Liu, D. W. C.; Thomas, J. H. Regulation of a Periodic Motor Program in *C. elegans*. *J. Neurosci.* **1994**, *14*, 1953–1962.
16. Allman, E.; Johnson, D.; Nehrke, K. Loss of the Apical V-ATPase a-Subunit VHA-6 Prevents Acidification of the Intestinal Lumen During a Rhythmic Behavior in *C. elegans*. *Am. J. Physiol.: Cell Physiol.* **2009**, *297*, C1071–C1081.
17. Nehrke, K. A Reduction In Intestinal Cell pH(i) Due to Loss of the *Caenorhabditis elegans* Na^+/H^+ Exchanger NHX-2 Increases Life Span. *J. Biol. Chem.* **2003**, *278*, 44657–44666.
18. Lee, S. K.; Li, W.; Ryu, S. E.; Rhim, T.; Ahnn, J. Vacuolar (H+)-ATPases in *Caenorhabditis elegans*: What Can We Learn about Giant H^+ Pumps from Tiny Worms? *Biochim. Biophys. Acta, Bioenerg.* **2010**, *1797*, 1687–1695.
19. Oka, T.; Toyomura, T.; Honjo, K.; Wada, Y.; Futai, M. Four Subunit a Isoforms of *Caenorhabditis elegans* Vacuolar H^+-ATPase—Cell-Specific Expression During Development. *J. Biol. Chem.* **2001**, *276*, 33079–33085.
20. Pfeiffer, J.; Johnson, D.; Nehrke, K. Oscillatory Transepithelial H^+ Flux Regulates a Rhythmic Behavior in *C. elegans*. *Curr. Biol.* **2008**, *18*, 297–302.
21. Sun, H. H.; Andresen, T. L.; Benjaminsen, R. V.; Almdal, K. Polymeric Nanosensors for Measuring the Full Dynamic pH Range of Endosomes and Lysosomes in Mammalian Cells. *J. Biomed. Nanotechnol.* **2009**, *5*, 676–682.
22. Clark, H. A.; Barker, S. L. R.; Brasuel, M.; Miller, M. T.; Monson, E.; Parus, S.; Shi, Z. Y.; Song, A.; Thorsrud, B.; Kopelman, R.; *et al.* Subcellular Optochemical Nanobiosensors: Probes Encapsulated by Biologically Localised Embedding (PEBBLEs). *Sens. Actuators, B* **1998**, *51*, 12–16.
23. Lim, S. F.; Riehn, R.; Ryu, W. S.; Khanarian, N.; Tung, C. K.; Tank, D.; Austin, R. H. *In Vivo* and Scanning Electron Microscopy Imaging of Upconverting Nanophosphors in *Caenorhabditis elegans*. *Nano Lett.* **2006**, *6*, 169–174.
24. Aylott, J. W. Optical nanosensors—An Enabling Technology for Intracellular Measurements. *Analyst* **2003**, *128*, 309–312.
25. Clark, H. A.; Hoyer, M.; Philbert, M. A.; Kopelman, R. Optical Nanosensors for Chemical Analysis Inside Single Living Cells. 1. Fabrication, Characterization, and Methods for Intracellular Delivery of PEBBLE Sensors. *Anal. Chem.* **1999**, *71*, 4831–4836.
26. Burns, A.; Sengupta, P.; Zedayko, T.; Baird, B.; Wiesner, U. Core/Shell Fluorescent Silica Nanopartictes for Chemical Sensing: Towards Single-Particle Laboratories. *Small* **2006**, *2*, 723–726.
27. Graber, M. L.; Dilillo, D. C.; Friedman, B. L.; Pastorizamunoz, E. Characteristics Of Fluoroprobes for Measuring Intracellular pH. *Anal. Biochem.* **1986**, *156*, 202–212.
28. Sarkar, D.; Mallick, A.; Haldar, B.; Chattopadhyay, N. Ratiometric Spectroscopic Response of pH Sensitive Probes: An Alternative Strategy for Multidimensional Sensing. *Chem. Phys. Lett.* **2010**, *484*, 168–172.
29. Haugland, R. *The Handbook: A Guide to Fluorescent Probes and Labeling Technologies*, 10th ed.; Invitrogen Corporation: Carlsbad, CA, 2005; p 1126.
30. Chauhan, V. M.; Burnett, G. R.; Aylott, J. W. Dual-Fluorophore Ratiometric pH Nanosensor with Tuneable pK(a) and Extended Dynamic Range. *Analyst* **2011**, *136*, 1799–1801.
31. Sun, H.; Almdal, K.; Andresen, T. L. Expanding the Dynamic Measurement Range for Polymeric Nanoparticle pH Sensors. *Chem. Commun.* **2011**, *47*, 5268–5270.
32. Benjaminsen, R. V.; Sun, H.; Henriksen, J. R.; Christensen, N. M.; Almdal, K.; Andresen, T. L. Evaluating Nanoparticle Sensor Design for Intracellular pH Measurements. *ACS Nano* **2011**, *5*, 5864–5873.
33. Ray, A.; Lee, Y.-E. K.; Elbez, R.; Kopelman, R. In *Targeted Nanosensor Aided Three-Dimensional pH Mapping in Tumor Spheroids Using Two-Photon Microscopy*, Conference on Multiphoton Microscopy in the Biomedical Sciences XII, San Francisco, CA, Jan 22−24, **2012**.

34. Schulz, A.; Wotschadlo, J.; Heinze, T.; Mohr, G. J. Fluorescent Nanoparticles for Ratiometric pH-Monitoring in the Neutral Range. *J. Mater. Chem.* **2010**, *20*, 1475–1482.
35. Ow, H.; Larson, D. R.; Srivastava, M.; Baird, B. A.; Webb, W. W.; Wiesner, U. Bright and Stable Core-Shell Fluorescent Silica Nanoparticles. *Nano Lett.* **2005**, *5*, 113–117.
36. McNamara, K. P.; Nguyen, T.; Dumitrascu, G.; Ji, J.; Rosenzweig, N.; Rosenzweig, Z. Synthesis, Characterization, and Application of Fluorescence Sensing Lipobeads for Intracellular pH measurements. *Anal. Chem.* **2001**, *73*, 3240–3246.
37. Bolanowski, M. A.; Russell, R. L.; Jacobon, L. A. Quantitative Measures of Aging in the Nematode *Caenorhabditis elegans*. 1. Population and Longitudinal-Studies of Two Behavioral Parameters. *Mech. Ageing Dev.* **1981**, *15*, 279–295.
38. Bolanowski, M. A.; Jacobson, L. A.; Russell, R. L. Quantitative Measures of Aging in the Nematode *Caenorhabditis elegans*. 2. Lysosomal Hydrolases as Markers of Senescence. *Mech. Ageing Dev.* **1983**, *21*, 295–319.
39. Herndon, L. A.; Schmeissner, P. J.; Dudaronek, J. M.; Brown, P. A.; Listner, K. M.; Sakano, Y.; Paupard, M. C.; Hall, D. H.; Driscoll, M. Stochastic and Genetic Factors Influence Tissue-Specific Decline in Ageing *C. elegans*. *Nature* **2002**, *419*, 808–814.
40. Smout, M. J.; Kotze, A. C.; McCarthy, J. S.; Loukas, A. A Novel High Throughput Assay for Anthelmintic Drug Screening and Resistance Diagnosis by Real-Time Monitoring of Parasite Motility. *PLoS Neglected Trop. Dis.* **2010**, 4.
41. Collins, J. J.; Huang, C.; Hughes, S.; Kornfeld, K. The Measurement and Analysis of Age-Related changes in *Caenorhabditis elegans*. *WormBook: The Online Review of C. elegans Biology*; Wormbook: Pasadena, CA, 2008; pp 1−21.
42. Wood, J. G.; Rogina, B.; Lavu, S.; Howitz, K.; Helfand, S. L.; Tatar, M.; Sinclair, D. Sirtuin Activators mimic Caloric Restriction and Delay Ageing in Metazoans. *Nature* **2004**, *430*, 686–689.
43. Ghafouri, S.; McGhee, J. D. Bacterial Residence Time in The Intestine of *Caenorhabditis elegans*. *Nematology* **2007**, *9*, 87–91.
44. Wendelhag, I.; Liang, Q.; Gustavsson, T.; Wikstrand, J. A New Automated Computerized Analyzing System Simplifies Readings and Reduces the Variability in Ultrasound Measurement of Intima-Media Thickness. *Stroke* **1997**, *28*, 2195–2200.
45. Kotula, P. G.; Keenan, M. R.; Michael, J. R. Automated Analysis of SEM X-ray Spectral Images: A Powerful New Microanalysis Tool. *Microsc. Microanal.* **2003**, *9*, 1–17.
46. Bland, J. M.; Altman, D. G. Statistical Methods For Assessing Agreement Between Two Methods of Clinical Measurement. *Lancet* **1986**, *1*, 307–310.
47. Geier, G.; Banaj, H. J.; Heid, H.; Bini, L.; Pallini, V.; Zwilling, R. Aspartyl Proteases in *Caenorhabditis elegans*—Isolation, Identification and Characterization by a Combined Use of Affinity Chromatography, Two-Dimensional Gel Electrophoresis, Microsequencing and Databank Analysis. *Eur. J. Biochem.* **1999**, *264*, 872–879.
48. Sifrim, D.; Castell, D.; Dent, J.; Kahrilas, P. J. Gastro-Oesophageal Reflux Monitoring: Review and Consensus Report on Detection and Definitions of Acid, Non-Acid, and Gas Reflux. *Gut* **2004**, *53*, 1024–1031.
49. Shannon, C. E. A Mathematical Theory of Communication. *Bell Syst. Tech. J.* **1948**, *27*, 379–423.
50. Nowell, M. A.; De Pomerai, D. I.; Pritchard, L. I. *Caenorhabditis elegans* as a Biomonitor for Immunological Stress in Nematodes. *Parasite Immunol.* **1999**, *21*, 495–505.